Proceedings of the 35th European Safety and Reliability & the 33rd Society for Risk Analysis Europe Conference
Edited by Eirik Bjorheim Abrahamsen, Terje Aven, Frederic Bouder, Roger Flage, Marja Ylönen

doi: 10.3850/978-981-94-3281-3_ESREL-SRA-E2025-P7679-cd

Towards Causality Graph Expansions For Local And Global Causal Assessment of Flow Network Models For Analytical System Resilience Explainability

Ivo Häring, Sebastian Ganter, Jörg Finger, Till Martini, Mirjam Fehling-Kaschek, Corinna Köpke, Alexander Stolz, Stefan Hiermaier

Fraunhofer EMI, Germany. E-mails: {haering; ganter; martini; fehling-kaschek; koepke; stefan.georg.fischer; stolz; hiermaier}@emi.fraunhofer.de

Network models of modern systems such as critical infrastructures, systems of systems, or human cyber-physical systems are key for their modelling, understanding, design, and analysis. Examples include electrical, communication, supply and transport networks, smart homes, or physical access systems. Graph, flow, or engineering-physical models allow by now to assess the influence of disruptions of single or more elements at different system levels to an increasing level of accuracy, transiency, and real time. Also, a plethora of metrics are available to assess system overall risk, e.g., system loss or resilience metrics. The present approach employs the concept of causal graphs and their quantification to reveal levels of dependencies of nodes, which can be extended to cover also edges. This is first conducted at the level of two nodes starting with direct causal dependency chains of first order, and then proposed to be extended to causal elementary models for three elements: chain, fork, and immorality. To assess to which degree two arbitrary nodes of the network are linked by a causal chain of first order, for simplicity a linear dependency model between the nodes is assumed, and its parameters are determined assessing the effect of critical possible risk and resilience weighted disruptions. In this way for each causal elementary graph its relevancy for the overall causal network can be ranked. If this is available for all causal building blocks a procedure can be given how to construct the overall causal graph bottom up avoiding cyclic and undirected structures. The proposed approach is described stepwise as well as equations are given for up to causal chains. The scaling of the approach is assessed. Best local causal models as well an overall causal model can be constructed. For an example the causal graph is constructed and discussed using first order causal chains.

Keywords: Network flow and transient model, causality graph, causal inference and quantification, chain, fork, immorality, local and global causal model, linear dependency model, risk and resilience weighting of disruptions.

1. Introduction

Critical infrastructures (CIs) are very successfully described using networks. This corresponds to their physical-technical realization at different scales. In the simplest case, networks are bus systems. It is assumed that all elements are interconnected and communicate with each other, exchanging energy, information or realizing material flows with assumed unlimited capacity. Bus system considerations have proved particularly successful in the field of power supply and communication.

For a general consideration, however, it is necessary to take the actual capacities of networks into account. There is a limit of information or material flow through transmission nodes, hubs, sources and sinks as well as edges. This also applies when intelligent protocols are based on the physical technical infrastructure, for instance in case of software defined communication networks (Agnew et al. 2024), industrial control systems of supply water grids (Etxezarreta et al. 2023), or windfarms internet of things designs (Mwangi et al. 2024). For example, data packets are exchanged through still available connections when following internet protocols. Similarly, gas (Zhang, Weng, and Qi 2023), water, oil or even electricity flows and fixing strategies (Jasiūnas et al. 2023) can only be adapted to the network capacity.

This paper examines the extent to which the cause of network failures can be determined based on an existing physical-technical network simulation. Aim is a contribution to the explainability of network disturbances or failures. The expectation is that causal explanations are better suited to generate narratives for the improvement of reliability and resilience of networks for internal and public communication through understanding which nodes and edges are causally responsible for expected failures, i.e., are main root cause candidates. To this end, it is explored whether causal information can be extracted from an existing complete technical simulative description of a supply network jointly with its risk and resilience assessment.

Therefore, the aim is to first select and define causal dependency relationships and describe them using causal graphs. An attempt will then be made to identify such causal graphs based on an existing network modeling and simulation as well as risk and resilience quantification. This is to be done locally, i.e., for few also distributed given nodes or edges, using simple causal elementary graphs for modelling their causal relationships: chains, forks and immoralities.

The aim is to determine the effect of damage, failure and disruption events, weighted with their probability on up to three local network elements using causal elementary graphs to single out selected potential causal relations. It is assumed that a complete modeling and simulation is available such that the relevancy of different causal graph models can be determined revealing the strength of causal impact relationships for local network elements. In an overall risk weighted combination their relevancy for the overall system is then used to determine an overall causal graph.

The paper is structured as follows. Section 2 discusses the difference between CI modelling perspectives: graph, network, Bayesian believe network (BBN), and Markov diagram, and finally causal graphs. In addition, the building blocks of causal networks are listed. More fundamentally, the previous use of causal analyses in the area of CI protection is discussed. Finally, the present approach is presented. Section 3 describes the proposed procedure of determining distributed local causal graphs and an overall causal graph based on a network flow simulation and risk and resilience analysis. Section 4 provides sample quantitative expressions for selected elementary causal graph building blocks with which the strength of causal dependencies of network elements can be determined and are ranked to build an overall causal graph. The feasibility of the methodology is assessed in terms of computation effort. Section 5 presents an application example. Section 6 concludes.

2. Technical network flow simulation versus graph abstractions and causal graphs

The section reviews various modeling and simulation perspectives on CI networks, parts of which are used to extract causal relationships.

For simplicity, we assume physical-technical networks that describe the transport of liquid or gaseous substances. Similar simulations can be applied to transport and energy systems. The conservation laws for mass, energy and momentum give rise to flow equations and together with the boundary conditions of the networks they define possible solutions. In the normal state or quasi-static state, i.e. with comparatively slow changes of overall system states, infrastructure networks are in equilibrium with regard to the quantities of material fed in and flowing out. Examples are gas networks (Hari et al. 2022), oil transport networks (Ali, Abdul-Majeed, and Al-Sarkhi 2024), water networks (Creaco et al. 2017), and transport networks (Dong, Shan, and Hwang 2022).

We consider various interruptions to the grids leading to transient behavior of the grids, i.e., time-dependent changes at shorter time scales. This may mean that consumption can no longer be covered. In this case, it is not possible to find a solution in which all consumers are supplied, see for instance for gas networks (Zalitis et al. 2022) (Kopustinskas et al. 2022) (Ganter et al. 2024).

In the case of incompressible liquids like freshwater, substance volume flow rates (volumes per time) are usually specified for substance sources and sinks. If gaseous transport mass flow is considered, consumers and sources can be described with (average) mass flow rate demands and in addition with minimum gas pressure requirements. In the gas case, it is therefore in general also necessary to switch off parts of the supply network in order to supply a residual network with sufficient gas at sufficient pressure.

In the following we assume that for a CI supply grid solutions are available for quasi-static as well as for transient behavior during disruptions leading again to quasi-static behavior.

One approach of causal analysis or discovery that operates without any *a priori* knowledge (Pearl 2022) (Zanga, Ozkirimli, and Stella 2022) is to first select a set of measurement data that depend on time and to consider them as realizations of random variables for which causal relations need to be determined. The next step is to normalize the data. Then a causal graph is constructed, also called causal qualitative analysis, see, e.g., (Kossakowski, Waldorp, and van der Maas 2021). The final step is to quantify the causal graph, also called causal inference, see, e.g., (Xu et al. 2023). With this a causal model of the data becomes available.

An example application of causal discovery to detection of root causes of delivery risks using domain knowledge is given in (Bo and Xiao 2024). However, when the described process is applied for instance to production data without using *a priori* knowledge it is difficult to identify such causal quantities as failure root causes in data of production processes (Qalaji et al. 2024), even when using different method options for each process step and for overall approach assessment production failure anomaly prediction capability.

In the case of supply grids modeled with flow simulation, when applying the causal discovery process, the throughput of nodes and edges could be used as random variables for which causal relations need to be determined using observed or simulated joint time histories in case of normal or disrupted operation. To the knowledge of the authors, no such approach has been tried so far.

Another approach could be to transform a supply grid flow simulation network into a causal graph, or at least a similar graphical structure. To this end we investigate how close supply grids are already to causal graphs.

Abstract graph models only consider nodes and directed edges, which could be based on abstractions of flow simulation grid models that also contain pumps, storage facilities, etc. Graphs determine a list of network-topology based metrics to assess resilience, e.g. centrality, connectedness, and redundancy (Ji et al. 2024). Network models suitable for flow simulation can be abstracted to graphs that also can be cyclic and that can have undirected (bidirectional) edges., e.g., if three nodes are connected with undirected pipelines this forms a cyclic graph. However, causal graph models require acyclic and directed graphs, which can be quantified to become causal inference models. So, there is no direct transition from networks suitable for flow simulation to causal graphs.

Also Bayesian Belief Networks (BBNs) can only be based on acyclic directed graphs, but allow a well-defined probabilistic interpretation as a compact representation of a joint distribution function of a complex system (Gaur et al. 2021). However, they are in general not causal graph models (Druzdzel and Simon 1993). Therefore, even from a general BBN, which can be assumed to be based on the flow model, causal graphs are not accessible.

In summary, there is no direct link between CI flow simulation network models and causal graphs, as the former can be cyclic and undirected, whereas the latter need to be acyclic and directed. Nevertheless, the flow network structure can be expected to be explorable to find causal relationships between nodes and edges in terms of causal graphs.

In the present case, instead of assuming an arbitrary variation of node or edge random variables as done in standard approaches just reviewed, the ambition of the paper is to consider a risk and resilience informed weighting wiggling driven by expectable disruptions. This will serve as an example how to use causality concepts in the domain of resilience of CIs (Häring et al. 2024).

3. Derivation of the Methodology

Instead of a transformation of the simulation flow network to a causal graph the idea is to determine it bottom up inductively by identifying elementary causal graphs, see Fig. 1.

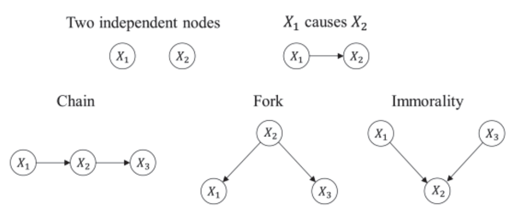

Fig. 1. Elementary causal graphs, see e.g. (Neal 2020).

The aim is furthermore to not only to use very basic causal relations, consisting of only two elements, out of the set of edges and nodes, see Fig. 1 for illustration. This is expected to allow for more subtle causal modelling, e.g., including the effect of cofounders, forks and colliders, to ensure sufficient complexity of the causal model.

Further idea is to use an overall risk ranking of potential disruption events on overall system level. Note that in standard approaches where data distributions for random variables are given, e.g., each random variable is wiggled around its mean value using its standard deviation as order of magnitude of the wiggle amplitude, and there is no relative weighting of random variables. However, we use systemic effects to identify and weight causal influence of single disruptions on relevancy of causal basic relations. This is expected to ensure that key causal relations are sufficient prominent in the final causal overall model.

The approach proposed reads:

1. Determine a flow network model of a CI.
2. Determine a set of boundary conditions for successful operation.
3. Determine a system loss function of the overall network considering short-term and long-term consequences, i.e. resilience informed consequences.
4. Determine the flow simulation solution of the network without any disruptions.
5. Generate a list of potential single disruption events.
6. Estimate the probabilities of the disruptions.
7. Determine for each disruption event the effect on the network for each node and edge as well as its resilience informed overall consequence.
8. Calculate the overall risk rank of each disruption using 6 and 7. Provide a critical overall risk threshold.
9. Generate a list of elementary causal graphical building blocks with up to three nodes.
10. Determine for all possible sets of two and three nodes of the flow grid network model the effect of all disruptions.
11. Considering disruptions with critical overall resilience-informed systemic risk define for each causal basic graph a metric to determine its relevancy.
12. Rank the set of nodes for each causal elementary model using the metric of 11. Provide a minimum critical value of the metric such that a dependency should be considered.
13. For each causal diagram type, rank its relevancy for overall causal graph building.
14. Using the ranked list of basic causal building blocks, combine the dependencies to the overall causal diagram while ensuring that causal graph model requirements are observed. If ambiguities arise use the ranking of identified elementary graphs as well as their internal ranking to determine how a causal dependency is considered.
15. Conduct the overall process till stability with respect to minor changes of the process steering parameters, e.g., loss function definition in 3, probability of disruption event estimates in 6, relative weighting of elementary diagrams in 13, as well as threshold values, e.g., critical resilience informed overall risk as introduced in 8 and minimum dependency metric as introduced in 12.

The question arises, how key steps of the proposed approach can be formalized to assess if the steps can be fulfilled in practical implementations.

4. Equations for Overall Risk-Supported Causal Graph Construction

Let $n_i, i = 1,2,\dots,N_n$ be a set of nodes and $e_{ij} = e_{i\to j}, i,j = 1,2,\dots,N_n$ be the corresponding set of directed edges, where $e_{ij} = 1$, if there is an edge from n_i to n_j and $e_{ij} = 0$, if not. Then define $s(n_i) < 0$ as maximum sink mass flow rate of node n_i, passive nodes as $s(n_i) = 0$, maximum source node flow rates as $s(n_i) > 0$, similarly minimum and maximum pressures p_{min} and p_{max} for sink and source nodes are defined. The capacity of maximum net mass flow rate through a node is $c(n_i) > 0$ and through a directed edge $c(e_{ij}) > 0$. If the network flow model with the above given network data and initial conditions is solvable then for each node the quasi-static pressure $p(n_i)$ and net mass flow rate $f(n_i)$ can be determined, as well as for each edge direction the flow rate $f(e_{ij})$.

To describe the effect of disruption events let $d_k, k = 1,2,\dots,N_d$ be a set of representative disruptions. Let $P(d_k)$ be the resilience aware probability by considering detection and prevention of the event d_k and $C(d_k)$ be its resilience-aware consequence by considering reduced consequences in case of fast recovery on system level, resulting in the overall risk value at system level of $R(d_k) = P(d_k)\, C(d_k)$. Let R_{crit} be a critical overall minimum risk threshold. Then

$p(n_i, d_k)$ is the pressure at the node n_i in case of the disruption d_k.

For simplicity, we determine in the following the dependence of nodes on each other only in case of single disruptions occurring as well as in terms of the change of pressure as random variable X at the nodes, see Fig 2. Let $(n_{\iota_1} n_{\iota_2})$ be a pair of nodes with $\iota_1, \iota_2 = 1,2, \ldots, N_n, \ \iota_1 \neq \iota_2$.

To model causal dependency, we assume the linear model

$$p(n_{\iota_2}, d_k) - p(n_{\iota_2}) = a_{\iota_1,\iota_2} + b_{\iota_1,\iota_2}\left(p(n_{\iota_1}, d_k) - p(n_{\iota_1}) \right), \qquad (1)$$

where a_{ι_1,ι_2} is a constant pressure offset and b_{ι_1,ι_2} is a constant direct proportionality factor relating pressure changes at node n_{ι_1} to changes at node n_{ι_2} that parametrizes the causal chain dependency of n_{ι_2} on n_{ι_1} of first order.

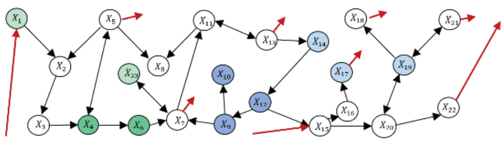

Fig. 2. Selection of sample sets of 2 (green) and 3 (blue) non-overlapping nodes for the evaluation of the relevance of the causal dependency chains of length 2 and 3. Boundary conditions are red. The darker the colors of nodes, the more likely it is that they will be confirmed by the flow simulation.

Using eq. (1) and assuming that the causal elementary graph describing that X_1 causes X_2 in Fig. 1 needs to be identified we compute for each combination $(n_{\iota_1}, n_{\iota_2})$ the related coefficients $(a_{\iota_1,\iota_2}, b_{\iota_1,\iota_2})$ using Chi-square minimization of

$$! \min = \mathrm{X}\left(a_{\iota_1\iota_2}, b_{\iota_1,\iota_2} ; \, n_{\iota_2}, n_{\iota_2} \right) = \qquad (2)$$

$$= \left(\sum_{\substack{k=1, \\ R(d_k) \\ \geq R_{crit}}}^{N_d} R(d_k)^q \left| p(n_{\iota_2}, d_k) - p(n_{\iota_2}) - a_{\iota_1\iota_2} - b_{\iota_1\iota_2}\left(p(n_{\iota_1}, d_k) - p(n_{\iota_1}) \right) \right|^q \right)^{\frac{1}{q}},$$

where between the absolute value lines of eq. (2) is just the lhs. of eq. (1) minus the rhs. of eq. (1), and $q > 0$, e.g., $q = 2$.

Now b_{ι_1,ι_2} of (2) can be used to assess the overall systemic risk and resilience weighted causal dependency strength of node n_{ι_2} on node n_{ι_1}. It is positive if on average over all disruption events d_k the pressure at node n_{ι_2} decreases if the pressure at node n_{ι_1} decreases. For the ranking of the direct causal relation of the node pairs $(n_{\iota_1}, n_{\iota_2})$, e.g., the expression $|b_{\iota_1,\iota_2}|$ is used to consider all possible dependency patterns.

Also, for constructing the overall causal graph the metric $|b_{\iota_1,\iota_2}|$ can be used to rank all causal connections $(n_{\iota_1}, n_{\iota_2})$ while considering a minimum threshold value of the dependency metric

$$\left| b_{\iota_1,\iota_2} \right| \geq b_{crit} > 0. \qquad (3)$$

To avoid undirected graphs always the pair $(n_{\iota_1}, n_{\iota_2})$ is selected with the higher dependency metric. Starting with the highest ranked pair further nodes are added. However, if a circular loop is observed, the node is not added to avoid constructing a cyclic directed graph. In this case the node pair that would close the loop is removed from the list of ranked nodes and not further considered.

To assess the effort needed for implementing this minimal realization of the 15-step approach scheme provided in section 2, first a conservative upper bound of the number of potential single disruptions is estimated as

$$N_d \leq N(\{d_k\}) = N_n + N_n(N_n - 1)/2 \sim N_n^2, \qquad (4)$$

which counts the options of removing single nodes and directed edges assuming that always bidirectional connections are realized.

The number of the potential direct causal relations for which the dependency strength metrics b_{ι_1,ι_2} need to be assessed using (2) is

$$N\left(\{(n_{\iota_1} n_{\iota_2})\}\right) = N_n(N_n - 1) \sim N_n^2, \qquad (5)$$

as the nodes do not interact with themselves, but all potential dependencies need to be assessed, see Fig. 3.

Regarding computational main effort, the computation of the resilience-informed consequences $C(d_k)$ of disruptions is expected to be dominating as it requires flow-grid simulations. We observe that the upper bound of the latter scale in the same way, see (4), as the number of minimization problems according to (2), which need to be solved for the computation of the dependency metrics, see eq. (5).

The present approach can be extended to the consideration of elementary causality graphs of 3-rd order in the following way. Instead of eq. (1) consider for triples $(n_{\iota_1}, n_{\iota_2}, n_{\iota_3})$, e.g. assessing the presence of causal chains according to Fig. 1, the following nested expression

$$p(n_{\iota_3}, d_k) - p(n_{\iota_3}) = a_{\iota_1,\iota_2,\iota_3} + b_{\iota_1,\iota_2,\iota_3}\left(p(n_{\iota_2}, d_k) - p(n_{\iota_2}) \right) = a_{\iota_1,\iota_2,\iota_3} +$$

$$b_{\iota_1,\iota_2,\iota_3}\Big(c_{\iota_1,\iota_2,\iota_3} + d_{\iota_1,\iota_2,\iota_3}\left(p(n_{\iota_1}, d_k) - p(n_{\iota_1})\right)\Big), \qquad (5)$$

where $a_{\iota_1,\iota_2,\iota_3}$, $b_{\iota_1,\iota_2,\iota_3}$, $c_{\iota_1,\iota_2,\iota_3}$ and $d_{\iota_1,\iota_2,\iota_3}$ are determined. As a joint metric of the relevancy of the elementary chain causal relationship based on eq. (5) $|b_{\iota_1,\iota_2,\iota_3}\, d_{\iota_1,\iota_2,\iota_3}|$ is a natural choice. Thus, besides a list of direct causal dependencies of 2-nd order, a ranked list of elementary causal chains of 3-rd order can be generated.

5. Application example

To evaluate (2), we choose the sample system of Fig. 3. Nodes n_1 and n_2 are source nodes with flow-in boundary conditions as described in section 3. All nodes $n_i,\ i = 1, 2, \ldots, N_n = 4$ have outflow boundary conditions to be served. We assume a bus like flow distribution such that each node connected to any of the two sources is supplied. For instance, n_4 is supplied by n_1 and n_2 and only fails if both sources fail. Node n_3 is only supplied by n_1.

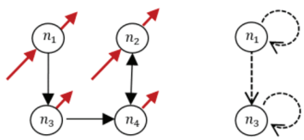

Fig. 3. CI network example with 4 nodes: (a) grid model, (b) causal model when only considering simple chains for assessment.

Table 1 lists the probabilities of disruption assumed, consequences in case of loss of nodes and resulting risks on system level using the notation introduced in section 3.

Table 1. Probabilities of node disruptions, consequences and risks on system level for sample system.

Dis-ruption	Ini-tial loss	Fur-ther nodes lost	All nodes lost $C(d_k)$	Proba-bility $P(d_k)$ $[a^{-1}]$	Risk $R(d_k)$ $[a^{-1}]$
d_1	n_1	n_3	2	$2 \cdot 10^{-4}$	$4 \cdot 10^{-4}$
d_2	n_2	-	1	10^{-5}	10^{-5}
d_3	n_3	-	1	10^{-6}	10^{-6}
d_4	n_4	-	1	10^{-6}	10^{-6}

We assume a critical risk threshold level of overall system loss of $R_{crit} = 5 \cdot 10^{-5} a^{-1}$ below of which risks are neglected. Hence, in equation (2) only the effects of the disruptions d_1 and d_2 are considered to compute the linear dependencies b_{ι_1,ι_2} between nodes n_{ι_1} and n_{ι_2}. Furthermore, we set $q = 1$ for the p-norm resulting in the modulus norm.

Table 2 gives the results for the linear dependencies between the nodes as matrix $\left[b_{\iota_1,\iota_2}\right]_{\iota_1,\iota_2=1,2,\ldots,N_d}$. For instance, $b_{1,2}$ is obtained from

$$!min = \sum_{k=1}^{2} R(d_k)\,|p(n_2, d_k) - p(n_2) - a_{12} - b_{12}(p(n_1, d_k) - p(n_1)| \qquad (5)$$
$$= 4 \cdot 10^{-4}|1 - 1 - a_{12} - b_{12}(0 - 1)| + 10^{-5}|0 - 1 - a_{12} - b_{12}(1 - 1)|,$$

which is equivalent to

$$!min = 40|1 - 1 - a_{12} - b_{12}(0 - 1)| + |0 - 1 - a_{12} - b_{12}(1 - 1)|,$$

$!min = 40|-a_{12} + b_{12}| + |-1 - a_{12}|$. Hence, we find $a_{12} = -1$ and $b_{12} = -1$ as in Table 2.

From (5) we realize that there are $2^4 = 16$ possible combinations of pressures if in (5) a pressure value of 1 is used in case node is supplied and 0 if node is not supplied. For $b_{1,2}$

$$!min = 40|0 - 1 - a_{13} - b_{13}(0 - 1)| + |1 - 1 - a_{13} - b_{13}(1 - 1)|,$$

$!min = 40|-1 - a_{13} + b_{13}| + |a_{13}|$.

Hence, we find $a_{13} = 0$ and $b_{13} = 1$. For b_{24}

$$!min = 40|1 - 1 - a_{24} - b_{24}(1 - 1)| + |1 - 1 - a_{24} - b_{24}(0 - 1)|,$$

$!min = 40|a_{24}| + |-a_{24} - b_{24}|$. Hence $a_{24} = b_{24} = 0$. For b_{41}

$$!min = 40|0 - 1 - a_{41} - b_{41}(1 - 1)| + |1 - 1 - a_{41} - b_{41}(1 - 1)|,$$

$!min = 40|-1 - a_{41}| + |a_{41}|$, which is independent of b_{41}. Hence b_{41} is arbitrary. Now for each entry type in Table 2 one example has been given. The other entries are computed similarly.

Table 2. Linear dependency matrix for example system.

b_{ι_1,ι_2}	ι_2			
ι_1	**1**	**2**	**3**	**4**
1	1	−1	1	a.
2	−1	a.	−1	0
3	0	−1	1	0
4	a.	a.	a.	a.

By inspection of Table 2, n_3 is linear dependent on n_1, i.e. $b_{13} = 1$, which is as expected from Fig. 3 through the directed connection from n_1 to n_3. Node n_1 does not depend on n_3 as there is no connection. Node n_4 does not depend on n_3 as the latter is not assumed to fail according to the critical system risk threshold assumed.

Node n_4 does not depend on n_1 as it is supplied by n_2. Also, as n_3 is assumed as not failing due to the critical systemic risk threshold assumed, n_4 will always be supplied independent of n_1. The computation allows for an arbitrary value $b_{14} =$ a. Whether n_1 depends on n_4 cannot be decided as b_{41} is found to be arbitrary, also not whether n_2 depends on n_4, and whether n_3 depends on n_4. The last three statements hold as n_3 is assumed to be never failing due to the systemic critical risk threshold assumed. Hence, the arbitrary entries also mark independence, however, in this case due the assumption that the failure of certain nodes needs not to be considered because the systemic risks are assumed to be negligible.

The value $b_{12} = -1$ can be interpreted such that the supply of n_2 decreases if n_1 is supplied, which contradicts the additional supply of n_2. In addition, n_2 has independent supply anyway. So, this value needs to be rejected as non-physical solution. Also, n_1 is independent of n_2 as it has its own supply. Similarly, n_2 is independent of n_3 as it has its own supply. Furthermore, n_3 is independence of n_2 as it is supplied by n_1. In all these cases the solutions $b_{12} = b_{32} = \mathrm{b}_{23} = -1$ can be rejected as not physical.

In addition, note that the node set $\{n_3, n_4, n_2\}$ contains a collider elementary graphical model, see Fig. 1, which also holds for $\{n_1, n_4, n_2\}$. In the latter case we take advantage that n_3 is not assumed to fail anyway. Hence, we can expect a behavior different than for a chain or a double chain, see Fig. 1.

The diagonal linear self-dependencies reflect for n_1 and n_3 their dependency on their own operation as there is no backup. However, n_2 is supplied by n_1, and n_4 even by n_1 and n_2.

Let us summarize the causal dependencies as identified form (2) when considering a simple chain of length two as basic causal model to collect information, a risk threshold excluding the consideration of the failure of 2 out of 4 nodes, and the modulus p-metric case. We find that the only causal dependency that can be extracted besides self-dependencies is that n_3 depends on n_1, see Fig. 3 right hand side.

This result as obtained from the minimization task of equation (2) is consistent with the assumptions and direct inspection, as we consider only single disruptions of nodes. Node n_1 only depends on own supply, n_2 and n_4 have redundant supply, thus showing no dependence on a single node failure. Node n_3 is only supplied if n_1 is operational. We emphasize the significant reduction of complexity of the dependencies when comparing the grid model and the causal graph model of Fig. 3.

5. Conclusions and Outlook

The paper has introduced options of constructing causal graphs locally and then globally from existing flow models of CIs. The bottom-up approach generates for each pair and triple of nodes a metric assessing the applicability of causal elementary diagrams. An explicit equation has been given using elementary causal chains of 2-nd order and been proposed for causal chains of 3-rd order. Ranked local causal diagrams weighted with a relative importance of elementary causal diagram types while avoiding undirected and cyclic graphs are proposed to construct overall causal graphs.

Due to the combinatorial scaling of the computational effort with the number of nodes in quartic order, it is expected that hyperparameters need to restrict the numbers of combinations, e.g., by using a critical overall resilience-informed risk threshold R_{crit}, and a limited number of local causal graphs, e.g., the10 % dominating ones.

Novelty of the approach is that disruption weighting reduces the causal dependencies to the most dominating ones utilizing that nodes are assessed to be relatively robust or redundant compared to others and/or their loss has limited systemic effect. This was also seen in the application example. It computed the causal graph of a 4-node network with 2 sources and in total 4 directed edges. Only the failure of 2 nodes was found to be relevant on system level. The causal graph reduced to a single chain dependence and 2 self-loops only. Linear dependency allowed to rank the causal dependencies using the modulus norm.

Future work planned is to implement the approach to larger grids and to use more elementary causal graph models with up to 3 nodes. For small CI grids the constructed graph can be assessed by humans. Results could also be benchmarked with causal graph models constructed automatically without any domain knowledge and if quantified be used to assess the relative contribution of nodes to observed failures, which could be compared to flow grid simulative results. The approach can be generalized to consider multiple disruption events, where higher order elementary causal diagrams are expected to become even more influential. Finally, also coupled grids could be considered.

Acknowledgement

Partial funding is acknowledged by the EU project eFORT with grant agreement ID: 101075665 (eFORT 2022-2026) as well as the EU MSCA doctorial network FOURIER with grand agreement number ID: 101169429, which started on 01.12.2024.

References

Agnew, D., S. Boamah, A. Bretas, and J. McNair. 2024. Network security challenges and countermeasures for software-defined smart grids: A survey. *Smart Cities* 7 (4):2131–81. doi:10.3390/smartcities7040085.

Ali, A. A., G. H. Abdul-Majeed, and A. Al-Sarkhi. 2024. Review of multiphase flow models in the petroleum engineering: Classifications, simulator types, and applications. *Arabian Journal for Science and Engineering.* doi:10.1007/s13369-024-09302-0.

Bo, S., and M. Xiao. 2024. Root cause attribution of delivery risks via causal discovery with reinforcement learning. *Algorithms* 17 (11):498. doi:10.3390/a17110498.

Creaco, E., A. Campisano, M. Franchini, and C. Modica. 2017. Unsteady flow modeling of pressure real-time control in water distribution networks. *Journal of Water Resources Planning and Management* 143 (9). doi:10.1061/(ASCE)WR.1943-5452.0000821.

Dong, B.-X., M. Shan, and B.-G. Hwang. 2022. Simulation of transportation infrastructures resilience: A comprehensive review. *Environmental science and pollution research international* 29 (9):12965–83. doi:10.1007/s11356-021-18033-w.

Druzdzel, M. J., and H. A. Simon. 1993. Causality in bayesian belief networks. In *Uncertainty in artificial intelligence, proceedings of the ninth conference*, 3–11.

eFORT. 2022-2026. Establishment of a framework for transforming current epes into a more resilient, reliable and secure system all over its value chain, eu-project, grant agreement id: 101075665. Accessed September 23, 2023. https://cordis.europa.eu/project/id/101075665.

Etxezarreta, X., I. Garitano, M. Iturbe, and U. Zurutuza. 2023. Software-defined networking approaches for intrusion response in industrial control systems: A survey. *International Journal of Critical Infrastructure Protection* 42:100615. doi:10.1016/j.ijcip.2023.100615.

Ganter, S., T. Martini, V. Kopustinskas, et al. 2024. A highly robust gas network simulation approach through an inherently solvable problem formulation for network states far from intended design points. *Applied Mathematical Modelling* 127:297–326. doi:10.1016/j.apm.2023.12.009.

Gaur, V., O. P. Yadav, G. Soni, and A. P. S. Rathore. 2021. A literature review on network reliability analysis and its engineering applications. *Proceedings of the Institution of Mechanical Engineers, Part O: Journal of Risk and Reliability* 235 (2):167–81. doi:10.1177/1748006X20962258.

Hari, S. K. K., K. Sundar, S. Srinivasan, A. Zlotnik, and R. Bent. 2022. Operation of natural gas pipeline networks with storage under transient flow conditions. *IEEE Transactions on Control Systems Technology* 30 (2):667–79. doi:10.1109/TCST.2021.3071316.

Häring, I., J. Rosin, S. Ganter, et al. 2024. Analytical resilience quantification approaches (resilience analytics) to classify and rank first principle risk and resilience modelling and simulation methods. In: *63-rd ESReDA seminar,* , 31–51. Luxembourg: Publications Office.

Jasiūnas, J., T. Heikkinen, P. D. Lund, and I. Láng-Ritter. 2023. Resilience of electric grid to extreme wind: Considering local details at national scale. *Reliability Engineering & System Safety* 232:109070. doi:10.1016/j.ress.2022.109070.

Ji, A., R. He, W. Chen, and L. Zhang. 2024. Computational methodologies for critical infrastructure resilience modeling: A review. *Advanced Engineering Informatics* 62:102663. doi:10.1016/j.aei.2024.102663.

Kopustinskas, V., B. Vamanu, S. Ganter, J. Finger, I. Häring, I. Zalitis, and L. Zemite. 2022. Gas network modelling to support pipeline hub area risk assessment study. In *Advances in modelling to improve network resilience: Proceedings of the 60th esreda seminar*, ed. R. Remenytė-Prescott, K. Sanderson, V. Kopustinskas and K. Simola, 159–62.

Kossakowski, J. J., L. J. Waldorp, and H. L. J. van der Maas. 2021. The search for causality: A comparison of different techniques for causal inference graphs. *Psychological methods* 26 (6):719–42. doi:10.1037/met0000390.

Mwangi, A., R. Sahay, E. Fumagalli, M. et al. 2024. Towards a software-defined industrial IoT-edge network for next-generation offshore wind farms: State of the art, resilience, and self-x network and service management. *Energies* 17 (12):2897. doi:10.3390/en17122897.

Neal, B. 2020. Introduction to causal inference from a machine learning perspective, lecture notes. Accessed 5.2.2025. https://www.bradyneal.com/Introduction_to_Causal_Inference-Dec17_2020-Neal.pdf.

Pearl, J. 2022. *Causality: Models, reasoning, and inference.* Cambridge: Cambridge University Press.

Qalaji, M., T. Jawad, I. Häring, and T. Bronx. 2024. Causal failure root cause detection in sensor production image and machine data. In *34-th* ESREL, 135–44.

Xu, S., Y. Ge, Y. Zhang, J. Ma, R. Guo, and J. Li. 2023. Causal explainable ai // causal inference on graphs. In *Machine learning for causal inference*, ed. S. Li and Z. Chu, 137–59. Cham: Springer International Publishing.

Zalitis, I., A. Dolgicers, L. Zemite, et al. 2022. Mitigation of the impact of disturbances in gas transmission systems. *International Journal of Critical Infrastructure Protection* 39:100569. doi:10.1016/j.ijcip.2022.100569.

Zanga, A., E. Ozkirimli, and F. Stella. 2022. A survey on causal discovery: Theory and practice. *International Journal of Approximate Reasoning* 151:101–29. doi:10.1016/j.ijar.2022.09.004.

Zhang, Y., W. Weng, and Q. Qi. 2023. Resilience assessment and enhancement methods of large-scale gas distribution networks against disruptions due to earthquakes. *Reliability Engineering & System Safety* 240:109583. doi:10.1016/j.ress.2023.109583.